JACS
JOURNAL OF THE AMERICAN CHEMICAL SOCIETY
Article
pubs.acs.org/JACS

Click Synthesis, Aggregation-Induced Emission, *E*/*Z* Isomerization, Self-Organization, and Multiple Chromisms of Pure Stereoisomers of a Tetraphenylethene-Cored Luminogen

Jian Wang,[†] Ju Mei,[†] Rongrong Hu,[‡] Jing Zhi Sun,*[,†] Anjun Qin,*[,†] and Ben Zhong Tang*[,†,‡]

[†]MoE Key Laboratory of Macromolecular Synthesis and Functionalization, Department of Polymer Science and Engineering, Zhejiang University, Hangzhou 310027, China

[‡]Department of Chemistry, Institute for Advanced Study, Institute of Molecular Functional Materials, State Key Laboratory of Molecular Neuroscience, and Division of Biomedical Engineering, The Hong Kong University of Science and Technology, Clear Water Bay, Kowloon, Hong Kong, China

Supporting Information

ABSTRACT: It has been difficult to decipher the mechanistic issue whether *E*/*Z* isomerization is involved in the aggregation-induced emission (AIE) process of a tetraphenylethene (TPE) derivative, due to the difficulty in the synthesis of its pure *E* and *Z* conformers. In this work, pure stereoisomers of a TPE derivative named 1,2-bis{4-[1-(6-phenoxyhexyl)-4-(1,2,3-triazol)yl]phenyl}-1,2-diphenylethene (BPHTATPE) are successfully synthesized. Both isomers show remarkable AIE effect ($\alpha_{AIE} \geq 322$) and high fluorescence quantum yield in the solid state (Φ_F 100%). The conformers readily undergo *E*/*Z* isomerization upon exposure to a powerful UV light and treatment at a high temperature (>200 °C). Such conformational change, however, is not observed under normal fluorescence spectrum measurement conditions, excluding the involvement of the *E*/*Z* isomerization in the AIE process of the TPE-based luminogen. The molecules of (*E*)-BPHTATPE self-organize into ordered one-dimensional nanostructures such as microfibers and nanorods that show obvious optical waveguide effect. BPHTATPE shows rich chromic effects, including mechano-, piezo-, thermo-, vapo-, and chronochromisms. Its emission peak is bathochromically shifted by simple grinding and pressurization and the spectral change is reversed by fuming with a polar solvent, heating at a high temperature, or storing at room temperature for some time. The multiple chromic processes are all associated with changes in the modes of molecular packing.

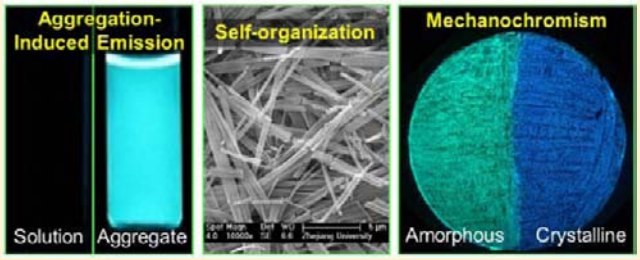

1. INTRODUCTION

Design and creation of efficient light emitters in the solid and aggregate states are of importance to the development of advanced optical and biomedical devices, such as organic light-emitting diodes (OLEDs) and fluorescent biosensors.[1] A formidable challenge in the area is the notorious photophysical effect of "aggregation-caused quenching" (ACQ): emission of a conventional luminophore is often weakened or even totally annihilated when its molecules are aggregated[2] due to energy transfer and the formation of excimers and exciplexes. Various chemical and physical approaches (e.g. attachment of alicyclic pendants, encapsulation by amphiphilic surfactants, and blending with transparent polymers) have been taken to alleviate the ACQ effect. These attempts, however, have met with only limited success, because they are basically working against an intrinsic process, i.e., the natural formation of aggregates of chromophores in the solid state.[3]

We have discovered an unusual photophysical phenomenon of "aggregation-induced emission" (AIE), which is exactly opposite to the ACQ process discussed above.[4−7] A series of propeller-shaped molecules, such as tetraphenylethene (TPE) and hexaphenylsilole (HPS), are nonluminescent in the dilute solutions but become highly emissive in the aggregate state. Thanks to the novel AIE effect, no elaborate work needs to be done to interrupt the aggregation processes of the luminogens. Instead, one can take advantage of aggregate formation to generate efficient solid emitters. The novel AIE effect permits the use of concentrated solutions of luminogens for sensing applications. The reliable and sensitive fluorescence turn-on nature of the AIE probes makes them promising candidates for applications in field screening, on-site trial, household testing, etc.[4,5] Efficient OLEDs can be readily fabricated using AIE luminogens as the active layers without complex engineering control.[6]

The useful AIE effect has stimulated much effort to study the intriguing photophysical process. As a result, a variety of AIE systems have been developed in the past decade.[4−7] Among the AIE luminogens developed so far, TPE is unique in that it is synthetically readily accessible (one-step reaction from

Received: September 21, 2011
Published: May 18, 2012

inexpensive reagents) and structurally easily manipulable (with numerous functional groups attachable through simple reactions).[7] Its exact AIE mechanism, however, remains to be deciphered. The issue involved is whether its AIE process is associated with the *E*/*Z* isomerization (EZI)[8] or the restriction of intramolecular rotation (RIR).[9] The EZI hypothesis assumes that, as TPE is a stilbene derivative, its excited states are nonradiatively annihilated by the EZI process in a dilute solution, whereas the decreased probability of EZI in an aggregate phase gives rise to an increase in the photoluminescence (PL) efficiency.[8] On the other hand, the RIR mechanism postulates that the PL of TPE in the solution is quenched by the dynamic intramolecular rotations of its multiple phenyl rotors against its ethylene stator, whereas the aggregate formation effectively suppresses the molecular motions, blocks the nonradiative energy dissipation channels, and opens up the radiative decay pathway.[4,9]

A correct mechanistic understanding of the AIE process is of academic value and has practical implications. It will guide our endeavors of structure design for the development of new AIE luminogens and assist our efforts to explore their potential technological applications. Although a wealth of experimental data in support of the RIR mechanism have been collected,[4] little is known about the involvement of the EZI process in an AIE system. Studying the EZI process requires pure *E* and *Z* isomers of an olefinic luminogen, whose synthesis, however, has been difficult, as the commonly used titanium-catalyzed McMurry coupling reaction only produces *E*/*Z* mixtures. We have attempted to use a palladium-catalyzed coupling reaction to prepare pure isomers.[10] The result was better but imperfect: the product was *Z*-rich but not 100% pure in conformation.

The great importance of drawing a clear mechanistic picture has motivated us to further tackle the synthetic difficulty and to prepare conformationally pure AIE luminogens. To enlarge the difference between the stereoisomers and to enhance their macroscopic separability, we designed in this work a triazole-functionalized TPE derivative named 1,2-bis{4-[1-(6-phenoxyhexyl)-4-(1,2,3-triazol)yl]phenyl}-1,2-diphenylethene (BPHTATPE) and accomplished its synthesis through the use of a copper-catalyzed Click reaction (Scheme 1).[11] As expected and much to our delight, the triazole-functionalization enabled the macroscopic separation of pure *E* and *Z* stereoisomers of the resultant BPHTATPE mixture by simple silica-gel column chromatography.

The successful acquisition of the pure stereoisomers of BPHTATPE permits us to study their conformational changes, if any, in their photophysical, especially AIE, processes using standard spectroscopic techniques such as NMR spectroscopy. An added bonus of the attachment of polar triazole pendants to the hydrophobic TPE core is the structural amphiphilicity of the resulting AIE luminogen, which endows its molecules with self-organizability and morphological tunability. In this paper, we report the conformational and morphological structures of BPHTATPE and its luminescent and chromatic properties in the solid state.

2. RESULTS AND DISCUSSION

Preparation of Pure Stereoisomers. While the McMurry coupling is a powerful and versatile reaction for the syntheses of TPE derivatives, the products are commonly mixtures of *E* and *Z* stereoisomers. Their separations by usual purification processes have been very difficult, if not impossible, due to the similarities in the molecular shapes and structural polarities of the steric conformers. Keeping this in mind, we thought that attaching large and polar moieties to a TPE core might bring about a big enough difference in the shape and polarity of the resultant TPE derivative to enable macroscopic separation of its stereoisomers.

Scheme 1. Synthesis of a BPHTATPE Mixture by "Click" Reaction and Isolation of Its Pure *E* and *Z* Conformers by Column Separation[a]

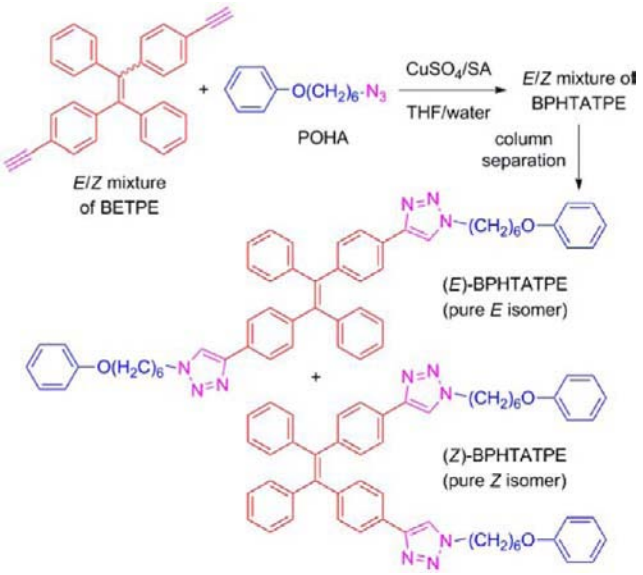

[a]BPHTATPE = 1,2-bis{4-[1-(6-phenoxyhexyl)-4-(1,2,3-triazol)yl]-phenyl}-1,2-diphenylethene, BETPE = 1,2-bis(4-ethynylphenyl)-1,2-diphenylethene, POHA = 6-(phenoxy)hexyl-azide, and SA = sodium ascorbate.

Along this line of consideration, we designed the structure of a functionalized TPE molecule and realized its preparation by the synthetic route shown in Scheme 1. A mixture of *E*/*Z* stereoisomers of 1,2-bis(4-ethynylphenyl)-1,2-diphenylethene (BETPE) prepared by McMurry coupling[12] was subjected to the alkyne−azide Click reaction with 6-(phenoxy)hexylazide (POHA) catalyzed by a mixture of $CuSO_4$/sodium ascorbate (SA) at room temperature. The reaction proceeded smoothly, giving an *E*/*Z* mixture of BPHTATPE in a high yield (89%).[11] The conformer mixture was separated by a routine silica-gel column using a dichloromethane (DCM)/acetone mixture as the eluent, affording the pure *E* and *Z* isomers as white and pale-yellow powders, respectively. The success in the isomer separation by the macroscopic technique of simple column chromatography proves that our structural design elaborated above has worked as expected.

The separated stereoisomers were characterized by various spectroscopic methods, from which satisfactory analysis data were obtained [Figures S1−S5, Supporting Information (SI)]. While the full ^{1}H NMR spectra of the isomers are given in Figure S2 in the SI, their partially magnified spectra in the aromatic region are depicted in Figure 1. The spectral profiles of the stereoisomers are similar. Closer examination, however, reveals that many of the resonance peaks of the *E* isomer are downfield-shifted from those of its *Z* counterpart. The most obvious spectral difference lies in the chemical shift region of 7.04−7.14 ppm. The *E* isomer resonates at δ 7.09 (Figure 1A), where the *Z* isomer is silent (Figure 1B). On the other hand, the *Z* isomer exhibits a big resonance peak at $\delta \approx 7.06$. These

dx.doi.org/10.1021/ja208883h | J. Am. Chem. Soc. 2012, 134, 9956−9966

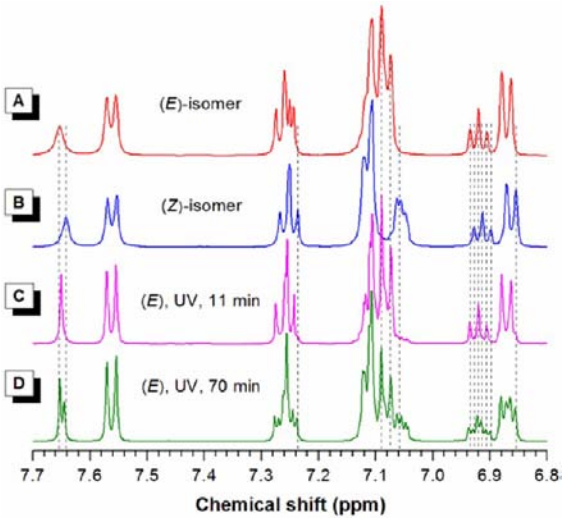

Figure 1. ^{1}H NMR spectra of (A) (*E*)-BPHTATPE, (B) (*Z*)-BPHTATPE, and (C, D) (*E*)-BPHTATPE after irradiation by a UV light of 365 nm for (C) 11 and (D) 70 min.

differences make it possible to monitor conformation changes of the isomers by NMR spectroscopy.

In addition to the spectroscopic techniques, we looked for other means to substantiate our structural assignments. We tried to grow single crystals of the isomers, but our effort was in vain. BETPE (a starting material) could crystallize, but the resultant crystals were mixtures of its *E* and *Z* isomers. We carefully inspected the crystals and found that they contained two distinct forms: smaller needles and bigger chunks. We picked up some of the needles and chunks from the cocrystal mixtures and analyzed their structures by X-ray diffraction (XRD). The XRD crystallography data reveal that the needles and chunks are the single crystals of *E* (CCDC 834092) and *Z* (CCDC 834091) stereoisomers of BETPE, respectively.[12] We carefully separated and collected sufficient amounts of the *E* and *Z* stereoisomers by hand and used them as starting materials to carry out model reactions using the same Click procedures (Scheme 2). The products obtained from the model reactions using BETPE with *E* and *Z* conformations gave NMR spectral data identical to those of the *E* and *Z* isomers separated from the BPHTATPE mixture by column chromatography (Scheme 1), respectively, thereby unambiguously corroborating their stereochemical structures.

Scheme 2. Syntheses of Pure Stereoisomers of BPHTATPE from Corresponding Pure Stereoisomers of BETPE by Click Reactions

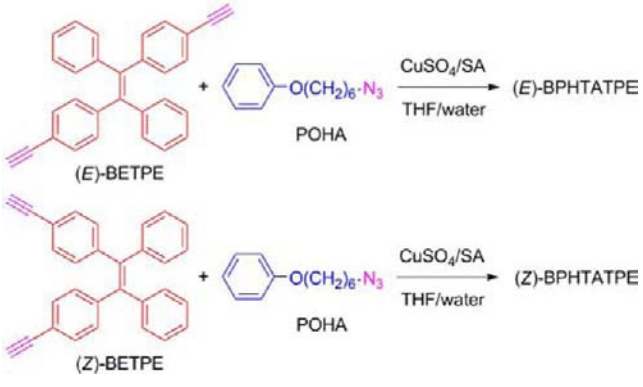

AIE Phenomena. After obtaining the pure *E* and *Z* isomers of BPHTATPE, we studied their photophysical processes. As can be seen from Figure S6 (SI), the dilute solution of the *E* isomer in THF shows an absorption maximum (λ_{max}) at ~332 nm. When water is mixed with THF, the absorption spectrum of the isomer remains practically unchanged until the amount of water in the aqueous mixture reaches a volume fraction (f_w) larger than 60 vol %. In the mixture with a high water content (f_w > 60%), the λ_{max} of the *E* isomer is blue-shifted to 319 nm. Meanwhile, the spectrum starts to show a tail in the long wavelength region. Similar spectral changes are observed in the case of the *Z* isomer (Figure S7, SI).

In the THF/water mixtures with high water content (f_w > 60%), the BPHTATPE molecules must have aggregated, due to their immiscibility with the polar media. The blue-shifts in the λ_{max} values of the *E* and *Z* stereoisomers ($\Delta\lambda_{max}$ > 10 nm) indicate that their molecules take a more twisted conformation in the aggregates, in agreement with the conclusion from a recent theoretical study.[13] The spectral tails in the long wavelength region, on the other hand, are caused by the Mie or light-scattering effect,[4−7] implying that the BPHTATPE aggregates are nanoparticles in dimensionality (vide infra).

Variations of the PL spectra of (*E*)-BPHTATPE with f_w in the THF/water mixtures are shown in panel A of Figure 2.

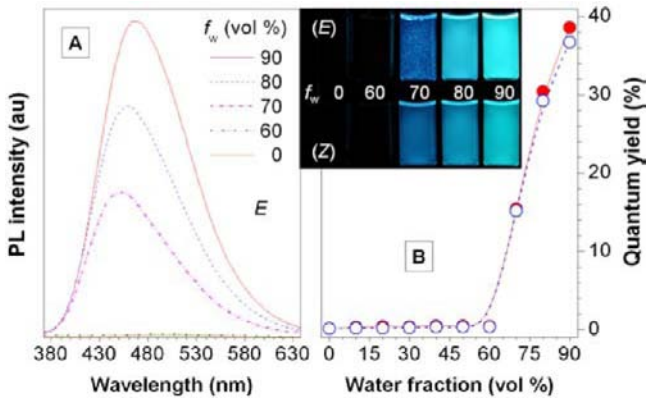

Figure 2. (A) Examples of PL spectra of (*E*)-BPHTATPE in the THF/water mixtures with different fractions of water (f_w); λ_{ex} = 332 nm, [BPHTATPE] = 10 μM. (B) Changes in the fluorescence quantum yields (Φ_F) of (*E*)- and (*Z*)-BPHTATPE with variations in f_w in the aqueous mixtures; Φ_F estimated using quinine sulfate in 0.05 M H_2SO_4 (Φ_F = 54.6%) as standard. (Inset) Fluorescence images of *E* and *Z* isomers of BPHTATPE in THF (f_w = 0%) and aqueous mixtures (f_w = 60−90%).

When excited by a UV light of 332 nm, the signals collected from the solution of the isomer are weak, and the plot of these signals vs wavelength is practically a flat line, indicating that the isomer is virtually nonfluorescent when it is molecularly dissolved in its good solvent. Not until the f_w is increased to >60 vol % has the spectrum started to change. The decreased solubility of the isomer in the aqueous mixture with high water content induces aggregate formation, which turns the fluorescence on. In other words, the emission is induced by aggregation, or the isomer is AIE active. When the f_w is further increased, the emission is continuously intensified, accompanying with a small red-shift in the spectrum. Similar AIE behavior is observed in the case of the *Z* isomer (Figure S7B, SI).

dx.doi.org/10.1021/ja208883h | J. Am. Chem. Soc. 2012, 134, 9956−9966

The formation of the luminogen aggregates in the aqueous mixtures with high water content was confirmed by dynamic light scattering (DLS) measurements (Figures S8−S11 in the SI). As can be seen from the data shown in Figures S8 and S9 (SI) for (*E*)-BPHTATPE, large aggregates with an average diameter (d) of ∼1400 nm are formed in the aqueous mixture with f_w = 70%. The size of the aggregates is decreased with an increase in the water content, as previously observed in many other AIE systems.[4−7] At f_w = 90%, the size of the aggregates is decrease to $d \approx 81$ nm. Similarly, the molecules of (*Z*)-BPHTATPE are aggregated in the aqueous mixtures with f_w > 70% (Figures S8 and S10 [SI]). In comparison to the size of the aggregates of the *E* isomer, the average size of the aggregates of the *Z* isomer formed at f_w = 70% is much smaller ($d \approx 527$ nm), although the sizes of the particles in the mixtures with higher f_w values are similar.

The formation of large aggregates in the f_w = 70% aqueous mixture is probably associated with a dynamic crystallization or organization process of the luminogen.[7b,14a] The larger d value of the aggregates of the *E* conformer than that of its *Z* counterpart indicates that the former is easier to crystallize or organize than the latter, in good agreement with the fact that the former is more readily isolated by the column separation process, although it is difficult to grow single crystals of high quality from the isomers. With an increase in f_w, the solvating power of the aqueous mixture is rapidly decreased. This makes the crystallization or organization process difficult to proceed and favors the formation of amorphous aggregates of smaller sizes.

The PL spectrum of (*E*)-BPHTATPE changes with time in the f_w = 70% aqueous mixture; it is intensified initially and weakened at later stages (Figure S12 in the SI). At f_w = 90%, however, almost no change in the PL spectrum was observed. The *Z* isomer shows similar behavior (Figure S13, SI). These PL spectral data support the discussion above. In the f_w = 70% mixture, the crystallization or organization process propagates with time. Accompanying the process, the PL is enhanced, as bigger crystals or assemblies are known to luminesce more efficiently.[4] Precipitation, however, occurs at some point when the crystals or assemblies grow to some critical sizes, which explains why the emission is weakened at the later stage. On the other hand, the fine amorphous particles do not grow with time at f_w = 90%,[4] which accounts for the time independence of the PL spectra in this mixture (Figures S12C and S13C [SI]). Since the PL spectrum changes with time in some aqueous mixtures (e.g., at f_w = 70%), in this work all the spectra were taken immediately after the samples were prepared.

The AIE feature of (*E*)-BPHTATPE is further verified by the trajectory of change in its fluorescence quantum yield (Φ_F) in the THF/water mixtures (Figure 2B). The Φ_F values of its solutions in the mixtures with $f_w \leq 60\%$ are negligibly small (down to 0.12%). In the mixture with f_w > 60%, aggregates commence to form. As a result of aggregate formation, the Φ_F value is swiftly increased. At f_w = 90%, the Φ_F value is boosted to 38.6%. Similar results are obtained in the case of the *Z* isomer. An α_{AIE} effect is defined as the ratio of the PL efficiencies of an AIE luminogen in the aggregate ($\Phi_{F,a}$) and solution ($\Phi_{F,s}$) states.[15] The α_{AIE} values for the *E* and *Z* isomers are found to be 322 and 334, respectively. It is remarkable that these values are much higher than that for HPS (α_{AIE} = 220), an iconic AIE luminogen.[16]

As can be seen from the photographs shown in the inset of Figure 2B, both the *E* and *Z* isomers of BPHTATPE emit a blue light in the THF/water mixture with f_w = 70%. The PL color is red-shifted to bluish-green when the water content in the aqueous mixture is increased to 90%. The absolute PL efficiencies of the two isomers in the solid state are measured to be 100% by the integrating sphere technique.[17] Repeated measurements over a long period (2 h) give the similarly high Φ_F values with little fluctuation (Figure S15, SI), verifying the reliability of the efficiency data and indicating that both of the stereoisomers are highly efficient emitters in the solid state and are photochemically stable under the integrating-sphere measurement conditions.

Not only the pure isomers but also their mixtures are AIE active. The UV, PL, and DLS data for an equimolar mixture of the *E* and *Z* isomers are shown in Figures S8, S11, S14, S16 and S17 in the SI as examples. The mixture is nonemissive with an insignificantly small Φ_F when dissolved in THF. Its emission is greatly enhanced when the water content in the THF/water mixture is increased to >60%. Its α_{AIE} value at f_w = 90% is 323, well comparable to those of its counterparts of pure stereoisomers. Similarly, the color of its emission is changed from blue to bluish-green when the water content is increased from 70% to 90%, as can be understood from the photographs shown in the inset of Figure S17 in the SI.

EZI vs RIR. The difference in the NMR spectra of the pure *E* and *Z* stereoisomers (cf., panels A and B in Figure 1) permits spectroscopic study of their EZI processes. As (*E*)-BPHTATPE is easier to obtain from the column separation of the reaction mixture, its EZI process is investigated in detail in this work. Irradiation of the *E* isomer with a UV lamp with a high power (1.10 mW/cm^2) readily yields the *Z* isomer (Table S1, SI), as evidenced by the photoinduced spectral changes (Figures S18 and S19 [SI]). After the *E* isomer is exposed to the irradiation for 11 min, new NMR signals, although weak in intensity, appear at δ 7.237, 7.059, and 6.855 (Figure 1C), where the *Z* stereoisomer resonates (cf., Figure 1B). The NMR signals are intensified when the UV irradiation is prolonged to 70 min, along with the appearance of new resonance peaks at δ 7.645, 6.930, and 6.900 (Figure 1D). As shown in Figure 3A, the *Z* fraction in the photogenerated *E*/*Z* mixture is rapidly increased to 35% in a nearly linear fashion in the first 50 min. Afterward, the EZI rate slows down. At 150 min, the fraction of the *Z*

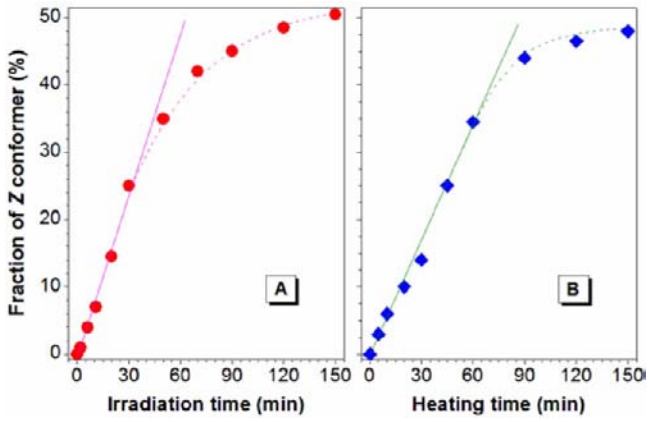

Figure 3. Variation in the *Z* fraction of BPHTATPE with time during the course of (A) irradiation of a chloroform-*d* solution of its *E* conformer by a UV light of 365 nm at room temperature or (B) heating of the solid powder of its *E* conformer at 203 °C under nitrogen.

dx.doi.org/10.1021/ja208883h | J. Am. Chem. Soc. 2012, 134, 9956−9966

isomer reaches 50.5%. The fractions calculated using the integrated areas of different resonance peaks give similar data within experimental errors (Table S1, SI).

It is known that the EZI process of an olefin can be caused not only by UV irradiation but also by thermal treatment.[18−20] The BPHTATPE isomers are resistant to thermal decomposition. The temperatures for 5% weight losses (T_d's) for the *E* and *Z* isomers are 374 and 273 °C (Figure S20, SI), while the melting points (T_m's) for the former and the latter are 202 and 163 °C, respectively. These thermal analysis data suggest that the *E* conformer takes a more regular molecular packing structure in the solid state. The wide gaps between the T_d and T_m values (ΔT = 110−172 °C) of the isomers allow the studies of their thermally induced EZI processes without worrying about the interference from the thermolysis process.

No change in the ^{1}H NMR spectrum is detected after the *E* isomer has been heated to and kept at 180 °C under nitrogen for 30 min (Figure S21, SI). However, when it is heated at 203 °C, a temperature above its T_m, the EZI process takes place, as revealed by the NMR data (Figure 4B as well as Figure S22 and Table S1 in the SI). The *Z* fraction is increased with an increase in the heating time (Figure 3B), although the rate is slower than that of its photoinduced EZI process. There is no detectable change in the ^{1}H NMR spectrum of the *Z* isomer when it has been heated to 165 °C and kept in the molten state for 30 min (Figure S21B, SI), indicating that the T_m is not high enough to activate the stereochemical reaction of this isomer. The EZI process, however, is triggered when the *Z* isomer is heated at a higher temperature of 203 °C (Figure 4D).

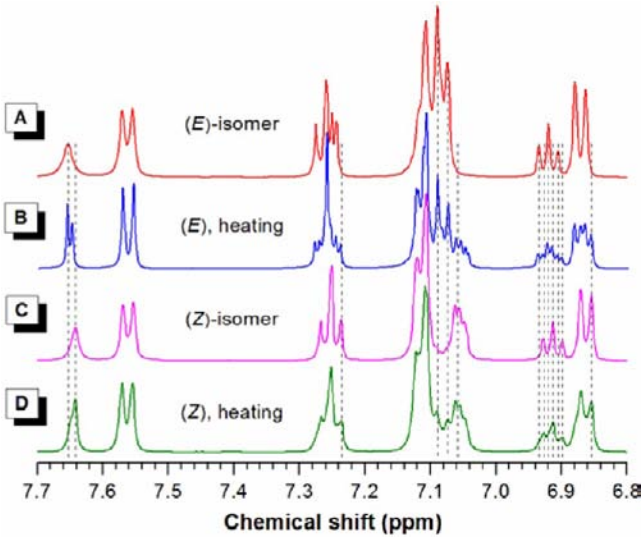

Figure 4. ^{1}H NMR spectra of (A) (*E*)-BPHTATPE (pure isomer), (B) (*E*)-BPHTATPE after heating at 203 °C for 90 min under nitrogen, (C) (*Z*)-BPHTATPE (pure isomer), and (D) (*Z*)-BPHTATPE after heating at 203 °C for 30 min under nitrogen.

The data presented above clearly show that the EZI process of BPHTATPE can be induced by the irradiation with a UV lamp of a high power (1.10 mW/cm^2) or the thermal treatment at a high temperature (203 °C). In the measurement of a PL spectrum, however, a spectrofluorometer is operating at much lower power (~52 μW/cm^2) and temperature (~20 °C). Does the EZI process occur under such mild conditions? To answer this question, a chloroform-*d* solution of the *E* conformer of BPHTATPE is put under continuous irradiation of the xenon lamp in the spectrofluorometer for 30 min at an excitation wavelength (λ_{ex}) of 332 nm. The ^{1}H NMR spectrum of the irradiated sample is identical to that of the original one (Figure S23A, SI), indicating that the EZI process has not occurred. Even when the λ_{ex} is changed to a shorter wavelength carrying a higher energy (254 nm), still no spectral change is detected. Similarly, no EZI process is observed after the *Z* conformer has been exposed to the irradiation by the xenon lamp in the spectrofluorometer (Figure S23C, SI).

The AIE phenomena of virtually all the AIE luminogens, in particular the TPE derivatives, have been observed under the PL spectral measurement conditions or under the excitation of a xenon lamp of low power at room temperature for a short while (commonly less than 1 min).[4−7] As stated above, the EZI processes of the *E* and *Z* isomers of BPHTATPE do not occur even after they have been irradiated for a much longer time (30 min). Clearly, the EZI process is not involved in the AIE process. The low power of the xenon lamp cannot break down the C═C bond, which is the critical initial step for the EZI process. The emission of BPHTATPE in the solution state is thus not quenched by the EZI process but the photoactivated intramolecular rotations of the aromatic rotors. The drastically boosted light emission in the aggregate state is caused by the restricted motions of the aromatic rotors. In other words, the RIR process is the mechanistic cause for the AIE activity of the TPE-based luminogen.

Self-Organization. During the study of the AIE process of (*E*)-BPHTATPE in the aqueous medium, white flocculent precipitates were found to appear in the THF/water mixture with f_w = 70% (vide ante). This implies the formation of some sort of organized structure.[21] We thus used the scanning electron microscope (SEM) to examine the morphological structure of the white precipitates. As can be seen from Figure 5A, the precipitates are one-dimensional microribbons with diameters down to a few hundred nanometers and lengths up to several tens of micrometers.

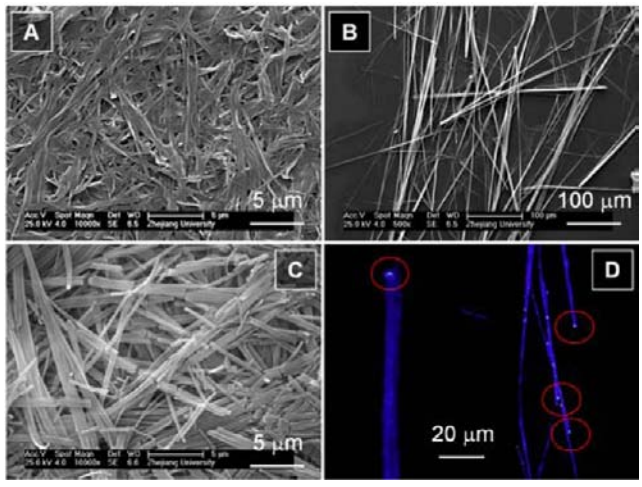

Figure 5. SEM microphotographs of the self-organized structures of (*E*)-BPHTATPE formed in the THF/water mixtures (A) at f_w = 70% instantly, (B) at f_w = 60% after standing for 1 week, and (C) the precipitate obtained after dropwise addition of hexane into a concentrated solution of (*E*)-BPHTATPE in chloroform. (D) Fluorescent image of the microfibers taken under a fluorescence microscope with a 337-nm excitation (sample from panel B).

dx.doi.org/10.1021/ja208883h | *J. Am. Chem. Soc.* 2012, 134, 9956−9966

Many larger microfibers are formed when a THF solution of (*E*)-BPHTATPE is diluted by a THF/water mixture with f_w = 60% and then kept standing under ambient conditions for 7 days (Figure 5B). The microfibers are visible to naked eyes, ~2 μm in diameter and several hundreds of micrometers in length. The microfibers may be used as building blocks for the construction of complex microstructures. Ordered assemblies are also formed when hexane, a poor solvent of the *E* isomer, is added dropwise into its concentrated solution in chloroform under slow stirring. The formed white precipitates are nanolumps with diameters of about 250 nm and lengths of tens of micrometers, as revealed by the SEM analysis (Figure 5C). This is evidently a rapid process for the fabrication of organic microstructures.

The organized microstructures of (*E*)-BPHTATPE, e.g., the microfibers, emit blue fluorescence upon excitation with a UV beam (Figure 5D). Glaring light emissions are seen at the ends of the microfibers (highlighted by the red circles in the figure), indicating that an optical waveguide effect is operating in the light transmission process of the microfibers. The waveguide effect is usually observed in an optically anisotropic system, such as crystalline assembly. The formation of microcrystals is thus the likely driving force for the (*E*)-BPHTATPE molecules to self-organize. The molecules of its *Z* isomer, on the other hand, can hardly form any microcrystalline structures, because of their irregular conformation.

Chromic Processes. Organic materials with tunable light-emitting behaviors have attracted much interest due to their potential applications as sensors, memories, security inks, logic-gate units, etc.[22,23] While luminescence from an emitter can be modulated by changing its molecular structure through chemical reactions or altering its molecular packing through external stimuli, the latter approach is advantageous in terms of simple procedures and engineering operability. A propeller shape is one of the most distinct structural features of an AIE luminogen. The packing structure of such molecules is susceptible to external perturbation, leading to a chromic response.[24] Since the molecule of BPHTATPE is also propeller shaped, it is expected to be chromically active. Indeed, it shows multiple chromic effects, including mechano-, piezo-, thermo-, vapo-, and chronochromisms.

The as-synthesized (*E*)-BPHTATPE is an off-white solid with a blue emission (Figure 6A). It changes to a pale-yellow powder with a bluish-green emission after grinding, showing a mechanochromic effect. Treating the ground sample at 120 °C for 1 min transforms it back to the off-white solid with the blue emission (noting that 120 °C is the lowest temperature at which a rapid thermochromic process occurs; see Figure S24 in the SI). The mechanochromism of the *E* isomer is further verified by the change in its PL spectrum. The emission peak of its as-obtained solid is located at 447 nm (Figure 6C). The corresponding CIE coordinate of the emitted light (x = 0.15, y = 0.12) is close to that of pure blue light, as defined by the National Television Standards Committee.[25] The isomer is thus an excellent blue emitter. Its emission peak is red-shifted to 477 nm by grinding. This suggests a morphological transition from crystalline to amorphous phase: an amorphous powder of an AIE luminogen often emits a redder light than its crystalline counterpart because its molecules usually take a more twisted conformation in the crystalline state than in the amorphous state.[4−7,13,24]

The as-synthesized (*Z*)-BPHTATPE is a pale-yellow solid with a bluish-green emission (Figure 6B). The color of its

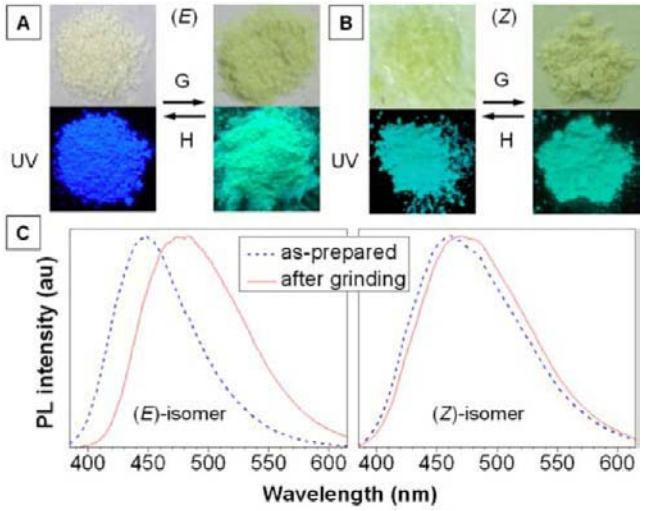

Figure 6. (A) Photographs of as-prepared (left) and ground (right) samples of (*E*)-BPHTATPE taken under room lighting (upper) and UV illumination (lower); *G* = grinding; *H* = heating (at 120 °C for 1 min). (B) Mechano- and thermochromic processes of (*Z*)-BPHTATPE, with the photographs arranged in the same order as in panel A. (C) PL spectra of (left) *E*- and (right) *Z*-conformers of BPHTATPE before and after grinding (λ_{ex} = 332 nm).

emission (460 nm) is redder than that of its *E* conformer (447 nm), implying that the solid is largely amorphous in nature, as discussed above.[4−7,14] Mechanical grinding of the solid causes little change in its physical appearance or emission color. As can be seen from Figure 6C, the grinding shifts its emission peak from 460 to 470 nm, with a change of merely 10 nm. This is reasonable because grinding a mainly amorphous solid should not make a great change in the morphologic structure and, hence, the fluorescence spectrum.

The different responses of the *E* and *Z* isomers to the grinding offer an opportunity to tune the extent of the chromic effect by changing the composition of the mixture of the two. Taking the mixtures with *E*/*Z* ratios of 8:2, 5:5, and 2:8 as examples, their emission peaks are shifted to 476, 474, and 472 nm by grinding, which respectively return to 452, 455, and 459 nm by heating (Figure S25, SI). The associated spectral shifts are 24, 19, 13 nm, respectively, clearly demonstrating that the bathochromic shift is readily tunable by the isomeric ratio.

Powder X-ray diffraction (XRD) pattern of the as-prepared solid of (*E*)-BPHTATPE shows intense and sharp reflection peaks (Figure 7A) due to its self-organized microcrystalline structure. After grinding, the XRD profile becomes broader with weaker reflection peaks (Figure 7B), indicating that the ordered assembly has been randomized to a largely amorphous mass. After heating at 120 °C, the sharp peaks in the XRD pattern are recovered (Figure 7C), manifesting that the ground sample has recrystallized into microcrystalline assembly upon the thermal treatment at the high temperature. The XRD data thus attest that the mechano- and thermochromisms are indeed associated with the morphology transformations between the crystalline and amorphous phases.

The XRD pattern of the as-obtained solid of the *Z* isomer is composed of a few blunt "peaks" (Figure 7E), meaning that it is mainly amorphous in nature or its crystallites are extremely small in size. The grinding almost completely amorphizes the solid, as reflected by the weak and broad XRD pattern of the ground sample. Heating at the high temperature again recovers

dx.doi.org/10.1021/ja208883h | *J. Am. Chem. Soc.* 2012, 134, 9956−9966

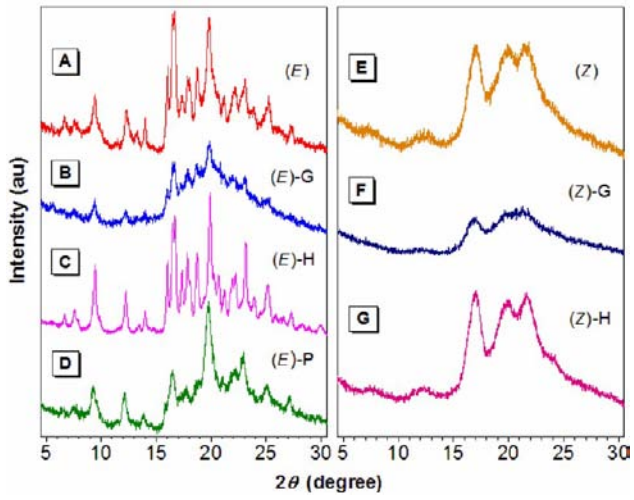

Figure 7. XRD patterns of as-prepared powders of (A) *E*-BPHTATPE and (E) *Z*-BPHTATPE and their samples after (B, F) grinding, (C, G) heating (at 120 °C for 1 min), and (D) pressurization (at 30 MPa for 1 min; for *E* isomer only). *G* = grinding, *H* = heating, and *P* = pressurization.

the morphological structure (Figure 7G). The XRD patterns of the *E* and *Z* isomers (cf., panels A and E in Figure 7) clearly demonstrate the differences in their crystallization capability, which account for their obviously different chromic behaviors.

Because of the more pronounced chromic effects of the *E* isomer, its chromic processes are studied in greater detail. Its emissions can be reversibly switched between two states (447 and 477 nm) by the grinding–heating cycle with almost no fatigue (Figure 8). Besides grinding, pressurization can also

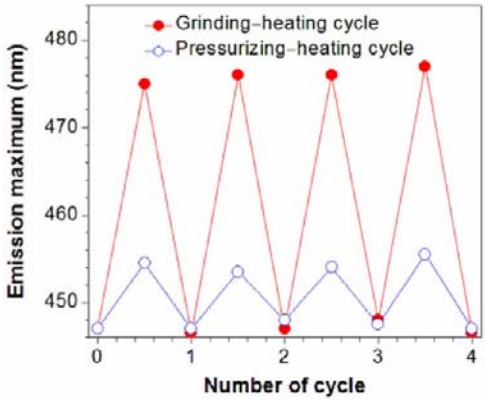

Figure 8. Reversible switching of emission of (*E*)-BPHTATPE by repeated grinding–heating (red line) or pressurization–heating (blue line) cycle; heating: 120 °C, 1 min; pressurization: 30 MPa, 1 min; λ_{ex} = 332 nm.

cause a red-shift in the PL spectrum of the isomer, although the shift is small (~8 nm; Figure S26, SI). The small change in the XRD pattern induced by the pressurization (Figure 7D) explains why the piezochromic effect is moderate in extent. The reversibility of the piezochromism is again superb (Figure 8). The great difference in the extent of the mechano- and piezochromic effects tells that, in comparison to compression (pressurization), shearing (grinding) is a more powerful force to bring about a larger change in the morphological structure and hence the emission spectrum.

The isomer shows a novel chronochromic phenomenon: its emission spectrum changes with time.[24,26] The emission peak of its ground sample is hypsochromically shifted by 8 nm after it has been kept under ambient conditions for 2 h (Figure 9A).

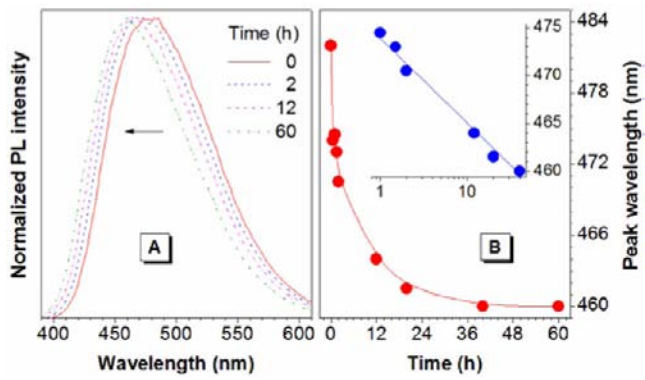

Figure 9. (A) Hypsochromic shift of PL spectrum of ground (*E*)-BPHTATPE with elapse of time at room temperature; λ_{ex} = 332 nm. (B) Plot of emission peak vs standing time. (Inset) Semilog relationship between peak wavelength and elapse of time.

The spectrum continues moving to shorter wavelengths as time elapses. The chronochromic process is very rapid at the beginning and levels off at the end, while in the middle region, the change in the PL peak follows a semilog relationship with time (Figure 9B). The chronochromism hints that the ground sample is in a metastable state, which transforms back to the thermodynamically stable crystalline state quickly at 120 °C and slowly at room temperature. The spontaneous recovery of morphological structure makes the AIE luminogen a unique self-healing optical material.

(*E*)-BPHTATPE further exhibits a solvent-dependent vapochromic effect. Its ground sample is sensitive to volatile polar solvents, such as chloroform, DCM, and THF. After exposure to the vapor of chloroform for as short as 1 min, the bluish-green emission of the ground sample of the *E* isomer is quickly reverted back to the blue emission of its crystals, owing to the fuming-induced crystallization (Figure 10A). When exposed to acetone, the vapochromism process becomes slower, with the blue emission being recovered in ~3 min.

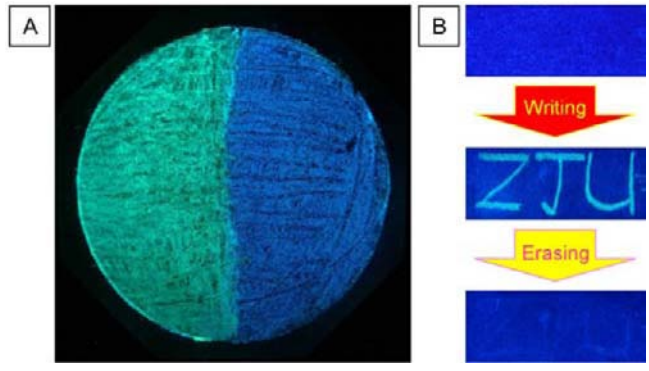

Figure 10. Fluorescence images of (A) a sphere of ground (*E*)-BPHTATPE with its right side fumed with chloroform vapor for 1 min, (B) a spray coating of the *E* isomer on a filter paper, then the letters of "ZJU" were written on the coating paper with a spatula, and subsequently the coating paper was treated by heating or vapor fuming (letters of "ZJU" becoming invisible or erased).

On the other hand, the ground sample is strongly resistant to a nonpolar solvent (e.g., hexane); fuming with the vapor of such a solvent for 10 min brings about no obvious change in the emission color. The distinct responses of the ground sample to the different fuming processes make it a promising chemosensor for discriminating solvents with different polarities.

It is envisioned that judicious utilization of the multiple chromic effects of (*E*)-BPHTATPE will lead to an array of technological applications. An example of such applications is demonstrated in Figure 10. When the powder of the isomer is sprayed on a filter paper as a thin film, it emits a blue light upon excitation with a hand-held UV lamp (Figure 10B). Letters of "ZJU" are written by gently scratching the film with a spatula, and due to the writing-induced mechanochromism the letters emit a bluish-green light. Heating at 120 °C or fuming with a polar solvent erases the letters by converting the light emission back to the background emission. No apparent change in the filter paper is visible under normal room lighting conditions in the whole process. The letters are invisible under room lighting but become visible with UV illumination. The isomer thus may be used as a security ink, and its reversible chromisms may be utilized to construct rewritable information storage systems.

3. CONCLUSIONS

Synthesis of stereopure conformers of TPE derivatives has been a difficult task. In this work, through rational structure design, we have successfully synthesized a pair of triazole-functionalized TPE derivatives, i.e., (*E*)- and (*Z*)-BPHTATPE, by the copper-catalyzed Click reaction and separated their pure conformers by the commonly used column chromatography technique. Their precise stereostructures are duly verified by the spectral characterizations and by the model reactions using stereopure BETPE isomers as the precursors, whose absolute conformations have been determined by the crystallographic analysis. Both of the *E* and *Z* isomers show pronounced AIE effects, with $\alpha_{AIE} \geq 320$ and $\Phi_F = 100\%$ in the solid state.

The acquisition of the pure stereoisomers has enabled us to study their EZI processes without ambiguity and gain useful insights into the AIE mechanisms of TPE-based luminogens. Our study reveals that the EZI process readily occurs when a BPHTATPE isomer is irradiated with a high flux UV lamp or heated at a high temperature. Under the conditions of normal PL spectral measurements, however, no EZI process can be detected even after the isomer has been put under irradiation by the xenon lamp in a standard spectrofluorometer for as long as 30 min. On the basis of the data collected in this work and the data obtained from our previous investigations,[4−7] we can conclude that the RIR process is the main cause for the novel AIE process of a TPE-based luminogen. The clear picture of the AIE mechanism will facilitate the structural design of new AIE luminogens and the exploration of their potential high-tech applications.[27,28]

The pure isomers have permitted the examination of their structure−morphology−function relationships. The symmetric and asymmetric shapes of the *E* and *Z* isomers significantly affect their molecular packing, with the former having much better organizability. The *Z* isomer exhibits poor assembling and crystallization capability, while the molecules of its *E* cousin can self-organize into ordered microstructures, such as microfibers and nanorods. Glaring light emmissions from the two ends of the microfibers occur upon photoexcitation. The optical waveguiding effect may allow the construction of advanced photonic devices employing the microfibers as the building blocks.

Both the conformers undergo multiple chromisms, with the *E* isomer showing more marked chromic effects, again owing to its better organizability or crystallinity. A simple grinding gives rise to a large bathochromic shift in its emission color (mechanochromism). Pressurization can also cause a red-shift in its emission color (piezochromism), though to a lesser extent. Heating of the ground or pressurized sample at a moderate temperature for a short while (120 °C, 1 min) can recover its emission color (thermochromism) with excellent reversibility. PL restoration of the ground sample proceeds with a semilog dependence on time at room temperature (chronochromism), exhibiting a novel optical self-healing effect. Fuming of the ground samples with the vapors of polar solvents can readily turn their emission colors back (vapochromism).

The multiple chromisms are associated with the distinctive structural feature of the AIE luminogens. The packing of their molecules is often loose, due to their propeller shape. Such molecular packing can be readily tuned, which in turn easily activates the phase transition or morphological transformation. The chromic responses of the AIE luminogens to the multiple external stimuli make the molecules promising candidates for advanced "smart" materials, which may find a wide variety of high-tech applications in miniature photonic devices, chemical sensors, biological probes, security inks, logic gates, optical displays, information storage, etc.

4. EXPERIMENTAL SECTION

Materials and Instrumentation. Chemicals, reagents, and solvents used in this work were all purchased from Acros, Alfa, and Aldrich, unless otherwise specified. THF was purified by the simple distillation from sodium benzophenone ketyl in an atmosphere of dry nitrogen immediately prior to use. Other solvents were purified by the standard procedures.

NMR spectra were measured on a DMX-500 spectrometer (Brulcer) in chloroform-*d* using TMS ($\delta = 0$) as the internal standard. IR spectra were taken on a Vector 22 spectrometer (Bruker). Elemental analysis was performed on a Thermo-Finnigan Flash EA1112. MALDI-TOF mass spectra were taken on a Waters GCT Premier GC-TOFMA mass spectrometer. Absorption spectra were measured on a Varian CARY 100 Bio spectrophotometer. PL spectra were recorded on a Perkin-Elmer LS 55 spectrofluorometer. Relative Φ_F values were estimated by using quinine sulfate in 0.05 M sulfuric acid (Φ_F = 54.6%) as standard. The absorbance of the solution was kept at ∼0.05 to avoid internal filter effect. Absolute Φ_F values were determined by a calibrated integrating sphere (see the SI for details).[17]

DLS measurements were conducted on a Brookhaven 90 Plus Particle Size Analyzer. Thermal stability was evaluated by taking thermograms on a Perkin-Elmer TGA 7 at 20 °C/min under nitrogen. T_m was measured on SGW X-4 micro melting point apparatus. EZI process was studied using a Spectroline UV lamp. Self-organization microstructure was checked by a SIRION-100 (FEI) SEM. Fluorescence micrographs were taken on a Carl-Zeiss LSM 10 META confocal laser scanning microscope. Powder XRD patterns were recorded on X'pert PRO, PANalytical, with Cu *Kα* radiation operating at 40 kV and 40 mA.

For the AIE measurement, a stock solution of a luminogen in THF (0.1 mM) was prepared. Aliquots of this stock solution

were transferred into volumetric flasks (10 mL), into which appropriate volumes of THF and water were added dropwise under vigorous stirring to give 10 μM solutions with different water contents (f_w = 0−90 vol %). UV and PL spectra were measured immediately after the solutions were prepared.

Synthesis and Characterization. The synthetic route to BPHTATPE is shown in Scheme 1. BETPE and POHA were prepared according to our previously published procedures,[5a] with all their characterization data matching the literature data. The model reactions (Scheme 2) were carried out in a similar manner. The detailed procedures for the preparation and separation of the *E* and *Z* isomers of BPHTATPE as well as their characterization data are given below.

Into a 50 mL Schlenk tube were added BETPE (0.380 g, 1.0 mmol), POHA (0.658 g, 3.0 mmol), and THF (10 mL). After complete dissolution of the starting materials, 2 mL of water and freshly prepared aqueous solutions of SA (1 M, 200 μL, 10 mol %) and $CuSO_4$ (1 M, 100 μL, 5 mol %) were added into the tube under vigorous stirring. The color of the solution turned to brown, orange, and then yellow. The reaction mixture was stirred at room temperature overnight. After the precipitate was filtered and THF was evaporated, the residue was extracted by DCM three times, washed with saturated ammonium chloride solution, brine, and water, and dried over magnesium sulfate. After filtration and solvent evaporation, the crude product was purified by a silica gel column using a DCM/acetone mixture (100:1 by vol) as the eluent. White (*E* isomer) and pale-yellow (*Z* isomer) powders were obtained in a total yield of 89.0% (0.729 g), with the *E*/*Z* ratio varied from batch to batch.

Characterization data for the E isomer: T_m: 201.5−202.5 °C. IR (KBr) ν (cm^{-1}): 3081, 2936, 1595, 1495, 1242, 1040, 821, 757, 696. ^{1}H NMR (500 MHz, $CDCl_3$) δ (TMS, ppm): 7.66 (s, 2H), 7.56 (d, 4H), 7.25 (t, 4H), 7.08 (m, 14H), 6.91 (t, 2H), 6.86 (d, 4H), 4.37 (t, 4H), 3.93 (t, 4H), 1.94 (m, 4H), 1.75 (m, 4H), 1.50 (m, 4H), 1.40 (m, 4H). ^{13}C NMR (125 MHz, $CDCl_3$) δ (ppm): 159.2, 147.8, 143.8, 143.7, 141.0, 132.1, 131.6, 129.7, 128.9, 128.1, 126.9, 125.2, 120.8, 119.7, 114.7, 67.7, 50.5, 30.5, 29.2, 26.4, 25.8. Anal. Calcd for $C_{54}H_{54}N_6O_2$: C, 79.19; H, 6.65; N, 10.26; Found: C, 79.06; H, 6.79; N, 10.30. HRMS (MALDI-TOF), *m*/*z* Calcd $C_{54}H_{54}N_6O_2$: 818.4308; Found: 818.4310.

Characterization data for the Z isomer: T_m: 162.0−164.0 °C. IR (KBr) ν (cm^{-1}): 3079, 2925, 1595, 1495, 1243, 1040, 810, 753, 694. ^{1}H NMR (500 MHz, $CDCl_3$) δ (TMS, ppm): 7.65 (s, 2H), 7.56 (d, 4H), 7.24 (t, 4H), 7.11 (m, 10H), 7.05 (m, 4H), 6.90 (t, 2H), 6.85 (d, 4H), 4.35 (t, 4H), 3.92 (t, 4H), 1.93 (m, 4H), 1.75 (m, 4H), 1.50 (m, 4H), 1.40 (m, 4H). ^{13}C NMR (125 MHz, $CDCl_3$) δ (ppm): 159.2, 147.8, 143.8, 143.7, 141.0, 132.1, 131.6, 129.6, 129.0, 127.9, 126.8, 125.3, 120.8, 119.7, 114.6, 67.6, 50.5, 30.5, 29.2, 26.4, 25.8. Anal. Calcd for $C_{54}H_{54}N_6O_2$: C, 79.19; H, 6.65; N, 10.26; Found: C, 78.91; H, 7.15; N, 9.67. HRMS (MALDI-TOF), *m*/*z* Calcd $C_{54}H_{54}N_6O_2$: 818.4308; Found: 818.4305.

■ ASSOCIATED CONTENT

Supporting Information

Text describing the procedures for measuring the absolute Φ_F in the solid state. Figures showing the FTIR, NMR, HRMS, UV, and PL spectra of the pure isomers of BPHTATPE and their mixtures, variations in the sizes and size distributions of their aggregates with f_w in aqueous mixtures, time dependences of their PL spectra, variations in the solid-state Φ_F of BPHTATPE with time, change in its Φ_F with f_w in the aqueous mixtures, NMR spectra of the BPHTATPE exposed to UV and xenon lamps and heated to high temperatures, its TGA thermograms, and mechano-, thermo-, and piezochromisms of its isomers and mixtures. This material is available free of charge via the Internet at http://pubs.acs.org.

■ AUTHOR INFORMATION

Corresponding Author

sunjz@zju.edu.cn (J.Z.S.); qinaj@zju.edu.cn (A.Q.); tangbenz@ust.hk (B.Z.T.)

Notes

The authors declare no competing financial interest.

■ ACKNOWLEDGMENTS

This work was partly supported by the Natural National Science Foundation of China (21074113, 50873086, 20974028, and 20974098), the Ministry of Science and Technology of China (2009CB623605), the Research Grants Council of Hong Kong (603509, HKUST2/CRF/10, and N_HKUST620/11), and the University Grants Committee of Hong Kong (AoE/P-03/08). B.Z.T. thanks the support from Cao Guangbiao Foundation of Zhejiang University. We thank Prof. Yuguang Ma and Dr. Ping Lu for the measurement of the solid-state quantum yields.

■ REFERENCES

(1) (a) Liu, B.; Dan, T.; Bazan, G. C. *Adv. Funct. Mater.* **2007**, *17*, 2432−2438. (b) Toal, S. J.; Jones, K. A.; Magde, D.; Trogler, W. C. *J. Am. Chem. Soc.* **2005**, *127*, 11661−11665. (c) Wu, Y.-T.; Kuo, M.-Y.; Chang, Y.-T.; Shin, C.-C.; Wu, T.-C.; Tai, C.-C.; Cheng, T.-H.; Liu, W.-S. *Angew. Chem., Int. Ed.* **2008**, *47*, 9891−9894. (d) Shimizu, M.; Takeda, Y.; Higashi, M.; Hiyama, T. *Angew. Chem., Int. Ed.* **2009**, *48*, 3653−3656. (e) Dong, J.; Solntsev, K. M.; Tolbert, L. M. *J. Am. Chem. Soc.* **2009**, *131*, 662−670. (f) Procopio, E. Q.; Mauro, M.; Panigati, M.; Donghi, D.; Mercandelli, P.; Sironi, A.; D'Alfonso, G.; De Cola, L. *J. Am. Chem. Soc.* **2010**, *132*, 14397−14399. (g) Nakamura, M.; Sanji, T.; Tanaka, M. *Chem.—Eur. J.* **2011**, *17*, 5344−5349. (h) Li, K.; Jiang, Y.; Ding, D.; Zhang, X.; Liu, Y.; Hua, J.; Feng, S.-S.; Liu, B. *Chem. Commun.* **2011**, *47*, 7323−7325. (i) Feng, J.; Tian, K.; Hu, D.; Wang, S.; Li, S.; Zeng, Y.; Li, Y.; Yang, G. *Angew. Chem., Int. Ed.* **2011**, *50*, 8072−8076. (j) Chen, Q.; Wang, J.-X.; Yang, F.; Zhou, D.; Bian, N.; Zhang, X.-J.; Yan, C.-G.; Han, B.-H. *J. Mater. Chem.* **2011**, *21*, 13554−13560. (k) Jin, X.-H.; Wang, J.; Sun, J.-K.; Zhang, H.-X.; Zhang, J. *Angew. Chem., Int. Ed.* **2011**, *50*, 1149−1153. (l) Perez, A.; Luis Serrano, J.; Sierra, T.; Ballesteros, A.; de Saa, D.; Barluenga, J. *J. Am. Chem. Soc.* **2011**, *133*, 8110−8113. (m) Ren, Y.; Kan, W. H.; Henderson, M. A.; Bomben, P. G.; Berlinguette, C. P.; Thangadurai, V.; Baumgartner, T. *J. Am. Chem. Soc.* **2011**, *133*, 17014−17026. (n) Xu, Y.; Chen, L.; Guo, Z.; Nagai, A.; Jiang, D. *J. Am. Chem. Soc.* **2011**, *133*, 17622−17625. (o) Shustova, N. B.; McCarthy, B. D.; Dincă, M. *J. Am. Chem. Soc.* **2011**, *133*, 20126−20129. (p) Lv, J.; Zhao, Y.; Li, G.; Li, Y.; Liu, H.; Li, Y.; Zhu, D.; Wang, S. *Langmuir* **2009**, *25*, 11351−11357.

(2) (a) Birks, J. B. *Photophysics of Aromatic Molecules*; Wiley: London, 1970. (b) Mullen, K.; Scherf, U. *Organic Light-Emitting Devices: Synthesis, Properties and Applications*; Wiley: Weinheim, 2006. (c) Grimsdale, A. C.; Chan, K. L.; Martin, R. E.; Jokisz, P. G.; Holmes, A. B. *Chem. Rev.* **2009**, *109*, 897−1091. (d) Shimizu, M.; Hiyama, T. *Chem.—Asian J.* **2010**, *5*, 1516−1531. (e) Wang, M.; Zhang, G.; Zhang, D.; Zhu, D.; Tang, B. Z. *J. Mater. Chem.* **2010**, *20*, 1858−1867. (f) Xia, J.; Wu, Y.-M.; Zhang, Y.-L.; Tong, B.; Shi, J.-B.; Zhi, J.-G.; Dong, Y.-P. *Imaging Sci. Photochem.* **2012**, *30*, 9−25.

(3) (a) Lee, S. H.; Jang, B. B.; Kafafi, Z. H. *J. Am. Chem. Soc.* **2005**, *127*, 9071−9078. (b) Chiang, C.-L.; Tseng, S.-M.; Chen, C.-T.; Hsu, C.-P.; Shu, C.-F. *Adv. Funct. Mater.* **2008**, *18*, 248−257. (c) Setayesh,

S.; Grimsdale, A. C.; Weil, T.; Enkelmann, V.; Muellen, K.; Meghdadi, F.; List, E. J. W.; Leising, G. *J. Am. Chem. Soc.* **2001**, *123*, 946−953. (d) Aldred, M. P.; Li, C.; Zhang, G.-F.; Gong, W. L.; Li, A. D. Q.; Dai, Y.; Ma, D.; Zhu, M.-Q. *J. Mater. Chem.* **2012**, *22*, 7515−7528.

(4) (a) Luo, J.; Xie, Z.; Lam, J. W. Y.; Cheng, L.; Chen, H.; Qiu, C.; Kwok, H. S.; Zhan, X.; Liu, Y.; Zhu, D.; Tang, B. Z. *Chem. Commun.* **2001**, 1740−1741. (b) Hong, Y.; Lam, J. W. Y.; Tang, B. Z. *Chem. Commun.* **2009**, 4332−4353. (c) Liu, J.; Lam, J. W. Y.; Tang, B. Z. *Chem. Rev.* **2009**, *109*, 5799−5867. (d) Hong, Y.; Lam, J. W. Y.; Tang, B. Z. *Chem. Soc. Rev.* **2011**, *40*, 5361−5388. (e) Yuan, C.; Xin, Q.; Liu, H.; Wang, L.; Jiang, M.; Tao, X. *Sci. Chin. Chem.* **2011**, *54*, 587−595. (f) Strassert, C. A.; Mauro, M.; De Cola, L. *Adv. Inorg. Chem.* **2011**, *63*, 47−103. (g) Wu, J.; Liu, W.; Ge, J.; Zhang, H.; Wang, P. *Chem. Soc. Rev.* **2011**, *40*, 3483−3495. (h) Kim, H. N.; Guo, Z.; Zhu, W.; Yoon, J.; Tian, H. *Chem. Soc. Rev.* **2011**, *40*, 79−93. (i) Chen, J.; Cao, Y. *Macromol. Rapid Commun.* **2007**, *28*, 1714−1742. (j) Wang, H.; Xie, Z.; Ma, Y.; Shen, J. *Sci. Chin. Chem.* **2007**, *50*, 433−452.

(5) (a) Wang, J.; Mei, J.; Yuan, W.; Lu, P.; Qin, A.; Sun, J.; Ma, Y.; Tang, B. Z. *J. Mater. Chem.* **2011**, *21*, 4056−4059. (b) Liu, Y.; Tang, Y.; Barashkov, N. N.; Irgibaeva, I. S.; Lam, J. W. Y.; Hu, R.; Birimzhanova, D.; Yu, Y.; Tang, B. Z. *J. Am. Chem. Soc.* **2010**, *132*, 13951−13953. (c) Liu, Y.; Deng, C.; Tang, L.; Qin, A.; Hu, R.; Sun, J.; Tang, B. Z. *J. Am. Chem. Soc.* **2011**, *133*, 660−663. (d) Peng, L.; Zhang, G.; Zhang, D.; Wang, Y.; Zhu, D. *Analyst* **2010**, *135*, 1779−1784. (e) Qian, Y.; Li, S.; Zhang, G.; Wang, Q.; Wang, S.; Xu, H.; Li, C.; Li, Y.; Yang, G. *J. Phys. Chem. B* **2007**, *111*, 5861−5868. (f) Hong, Y.; Meng, L.; Chen, S.; Leung, C. W. T.; Da, L.; Faisal, M.; Silva, D.-A.; Liu, J.; Lam, J. W. Y.; Huang, X.; Tang, B. Z. *J. Am. Chem. Soc.* **2012**, *134*, 1680−1689. (g) Qin, W.; Ding, D.; Liu, J.; Yuan, W. Z.; Hu, Y.; Liu, B.; Tang, B. Z. *Adv. Funct. Mater.* **2012**, *22*, 771−779.

(6) (a) Yu, G.; Yin, S.; Liu, Y.; Chen, J.; Xu, X.; Sun, X.; Ma, D.; Zhan, X.; Peng, Q.; Shuai, Z.; Tang, B. Z.; Zhu, D.; Fang, W.; Luo, Y. *J. Am. Chem. Soc.* **2005**, *127*, 6335−6346. (b) Chen, H.; Lam, J. W. Y.; Luo, J.; Ho, Y.; Tang, B. Z.; Zhu, D.; Wong, M.; Kwok, H. S. *Appl. Phys. Lett.* **2002**, *81*, 574−576. (c) Zhao, Z.; Chen, S.; Chan, C. Y. K.; Lam, J. W. Y.; Jim, C. K. W.; Lu, P.; Chang, Z.; Kwok, H. S.; Qiu, H.; Tang, B. Z. *Chem.—Asian J.* **2012**, *7*, 484−488.

(7) (a) Qin, A.; Lam, J. W. Y.; Tang, L.; Jim, C. K. W.; Zhao, H.; Sun, J.; Tang, B. Z. *Macromolecules* **2009**, *42*, 1421−1424. (b) Dong, Y.; Lam, J. W. Y.; Qin, A.; Liu, J.; Li, Z.; Tang, B. Z.; Sun, J.; Kwok, H. S. *Appl. Phys. Lett.* **2007**, *91*, 011111−1−3. (c) Zhao, Z.; Lam, J. W. Y.; Tang, B. Z. *Curr. Org. Chem.* **2010**, *14*, 2109−2131. (d) Jiang, Y.-H.; Wang, Y.; Hua, J.-L.; Tang, J.; Li, B.; Qian, S.; Tian, H. *Chem. Commun.* **2010**, *46*, 4689−4691.

(8) (a) Schilling, C. L.; Hilinski, E. F. *J. Am. Chem. Soc.* **1988**, *110*, 2296−2298. (b) Shultz, D. A.; Fox, M. A. *J. Am. Chem. Soc.* **1989**, *111*, 6311−6320. (c) Simeonov, A.; Matsushita, M.; Juban, E. A.; Thompson, E. H. Z.; Hoffman, T. Z.; Beuscher, A. E., IV; Taylor, M. J.; Wirsching, W. R.; McCusker, J. K.; Stevens, R. C.; Millar, D. P.; Schultz, P. G.; Lerner, R. A.; Janda, K. D. *Science* **2000**, *290*, 307−313. (d) Waldeck, D. H. *Chem. Rev.* **1991**, *91*, 415−436. (e) Saltiel, J.; D'Agostino, J. T. *J. Am. Chem. Soc.* **1972**, *94*, 6445−6455.

(9) (a) Zhao, Z.; Wang, Z.; Lu, P.; Chan, C. Y. K.; Liu, D.; Lam, J. W. Y.; Sung, H. H. Y.; Williams, I. D.; Ma, Y.; Tang, B. Z. *Angew. Chem., Int. Ed.* **2009**, *48*, 7608−7611. (b) Li, Z.; Dong, Y. Q.; Lam, J. W. Y.; Sun, J.; Qin, A.; Häußler, M.; Dong, Y. P.; Sung, H. H. Y.; Williams, I. D.; Kwok, H. S.; Tang, B. Z. *Adv. Funct. Mater.* **2009**, *19*, 905−917. (c) Pu, K. Y.; Liu, B. *Adv. Funct. Mater.* **2009**, *19*, 277−284. (d) Peng, Q.; Yi, Y.; Shuai, Z.; Shao, J. *J. Am. Chem. Soc.* **2007**, *129*, 9333−9339. (e) Yeh, H. C.; Yeh, S. J.; Chen, C. T. *Chem. Commun.* **2003**, 2632−2633. (f) You, Y.; Huh, H. S.; Kim, K. S.; Lee, S. W.; Kim, D.; Park, S. Y. *Chem. Commun.* **2008**, 3998−4000.

(10) Tseng, N.-W.; Liu, J.; Ng, J. C. Y.; Lam, J. W. Y.; Sung, H. H. Y.; Williams, I. D.; Tang, B. Z. *Chem. Sci.* **2012**, *3*, 493−497.

(11) (a) Rostovtsev, V. V.; Green, L. G.; Fokin, V. V.; Sharpless, K. B. *Angew. Chem., Int. Ed.* **2002**, *41*, 2596−2599. (b) Qin, A.; Lam, J. W. Y.; Tang, B. Z. *Macromolecules* **2010**, *43*, 8693−8702. (c) Qin, A.; Lam, J. W. Y.; Tang, B. Z. *Chem. Soc. Rev.* **2010**, *39*, 2522−2544.

(12) Hu, R.; Lam, J. W. Y.; Sung, H. H. Y.; Williams, I. D.; Yue, Z.; Wong, K. S.; Yuen, M. M. F.; Tang, B. Z. *Polym. Mater. Sci. Eng.* **2011**, *105*, 264−265.

(13) Li, M. C.; Hayashi, M.; Lin, S. H. *J. Phys. Chem. A* **2011**, *115*, 14531−14538.

(14) (a) Dong, Y.; Lam, J. W. Y.; Qin, A.; Sun, J.; Liu, J.; Li, Z.; Sun, J.; Sung, H. H. Y.; Williams, I. D.; Kwok, H. S.; Tang, B. Z. *Chem. Commun.* **2007**, 3255−3257. (b) Li, Z.; Dong, Y.; Mi, B.; Tang, Y.; Häussler, M.; Tong, H.; Dong, Y.; Lam, J. W. Y.; Ren, Y.; Sung, H. H. Y.; Wong, K. S.; Gao, P.; Williams, I. D.; Kwok, H. S.; Tang, B. Z. *J. Phys. Chem. B* **2005**, *109*, 10061−10066. (c) Tong, H.; Dong, Y.; Häussler, M.; Hong, Y.; Lam, J. W. Y.; Sung, H. H. Y.; Williams, I. D.; Kwok, H. S.; Tang, B. Z. *Chem. Phys. Lett.* **2006**, *428*, 326−330. (d) Zhao, Z.; Chen, S.; Lam, J. W. Y.; Wang, Z.; Lu, P.; Mahtab, F.; Sung, H. H. Y.; Williams, I. D.; Ma, Y.; Kwok, H. S.; Tang, B. Z. *J. Mater. Chem.* **2011**, *21*, 7210−7216.

(15) Zhao, Z.; Chen, S.; Shen, X.; Faisal, M.; Yu, Y.; Lu, P.; Lam, J. W. Y.; Kwok, H. S.; Tang, B. Z. *Chem. Commun.* **2010**, *46*, 686−688.

(16) Chen, J.; Law, C. W.; Lam, J. W. Y.; Dong, Y. P.; Lo, S. F.; Williams, I. D.; Zhu, D.; Tang, B. Z. *Chem. Mater.* **2003**, *15*, 1535−1546.

(17) Kawamura, Y.; Sasabe, H.; Adachi, C. *Jpn. J. Appl. Phys.* **2004**, *43*, 7729−7730.

(18) Momotake, A.; Arai., T. *J. Photochem. Photobiol. C* **2004**, *5*, 1−25.

(19) Sanchez, A. M.; Barra, M.; de Rossi, R. H. *J. Org. Chem.* **1999**, *64*, 1604−1609.

(20) (a) Arai, T.; Tokumaru, K. *Chem. Rev.* **1993**, *93*, 23−39. (b) Salem, L. *Acc. Chem. Res.* **1979**, *12*, 87−92.

(21) (a) Zhao, Z.; Liu, D.; Mahtab, F.; Xin, L.; Shen, Z.; Yu, Y.; Chan, C. Y. K.; Lu, P.; Lam, J. W. Y.; Sung, H. H. Y.; Willians, I. D.; Yang, B.; Ma, Y.; Tang, B. Z. *Chem.—Eur. J.* **2011**, *17*, 5998−6008. (b) Xu, B.; He, J.; Dong, Y.; Chen, F.; Yu, W.; Tian, W. *Chem. Commun.* **2011**, *47*, 6602−6604. (c) Li, D.-M.; Zheng, Y.-S. *J. Org. Chem.* **2011**, *76*, 1100−1108. (d) Hirose, T.; Higashiguchi, K.; Matsuda, K. *Chem.—Asian J.* **2011**, *6*, 1057−1063. (e) Dai, Q.; Liu, W.; Zeng, L.; Lee, C.-S.; Wu, J.; Wang, P. *CrystEngComm* **2011**, *13*, 4617−4624.

(22) (a) Ning, Z.; Chen, Z.; Zhang, Q.; Yan, Y.; Qian, S.; Cao, Y.; Tian, H. *Adv. Funct. Mater.* **2007**, *17*, 3799−3807. (b) Kishimura, A.; Yamashita, T.; Yamaguchi, K.; Aida, T. *Nat. Mater.* **2005**, *4*, 546−549. (c) Irie, M.; Fukaminato, T.; Sasaki, T.; Tamai, N.; Kawai, T. *Nature* **2002**, *420*, 759−760. (d) Sagara, Y.; Kato, T. *Angew. Chem., Int. Ed.* **2011**, *50*, 9128−9132. (e) Teng, M.-J.; Jia, X.-R.; Yang, S.; Chen, X.-F.; Wei, Y. *Adv. Mater.* **2012**, *24*, 1255−1261. (f) Chi, Z.; Zhang, X.; Xu, B.; Zhou, X.; Ma, C.; Zhang, Y.; Liu, S.; Xu, J. *Chem. Soc. Rev.* **2012**, *41*, 3878−3896.

(23) (a) Dong, Y. Q.; Lam, J. W. Y.; Li, Z.; Tong, H.; Dong, Y. P.; Feng, X. D.; Tang, B. Z. *J. Inorg. Organomet. Polym. Mater.* **2005**, *15*, 287−291. (b) Fan, X.; Sun, J.; Wang, F.; Chu, Z.; Wang, P.; Dong, Y. Q.; Hu, R.; Tang, B. Z.; Zou, D. *Chem. Commun.* **2008**, 2989−2991. (c) Sagara, Y.; Mutai, T.; Yoshikawa, I.; Araki, K. *J. Am. Chem. Soc.* **2007**, *129*, 1520−1521. (d) Teng, M.; Jia, X.; Chen, X.; Ma, Z.; Wei, Y. *Chem. Commun.* **2011**, *47*, 6078−6080. (e) Kunzelman, J.; Kinami, M.; Crenshaw, B. R.; Protasiewicz, J. D; Weder, C. *Adv. Mater.* **2008**, *20*, 119−122. (f) Chung, J. W.; You, Y.; Huh, H. S.; An, B. K.; Yoon, S. J.; Kim, S. H.; Lee, S. W.; Park, S. Y. *J. Am. Chem. Soc.* **2009**, *131*, 8163−8172. (g) Dou, C.; Chen, D.; Iqbal, J.; Yuan, Y.; Zhang, H.; Wang, Y. *Langmuir* **2011**, *27*, 6323−6329.

(24) (a) Mei, J.; Wang, J.; Qin, A.; Zhao, H.; Yuan, W.; Zhao, Z.; Sung, H. H. Y.; Deng, C.; Zhang, S.; Williams, I. D.; Sun, J.; Tang, B. Z. *J. Mater. Chem.* **2011**, *22*, 4290−4298. (b) Xu, B.; Chi, Z.; Zhang, J.; Zhang, X.; Li, H.; Li, X.; Liu, S.; Zhang, Y.; Xu, J. *Chem.—Asian J.* **2011**, *6*, 1470−1478. (c) Luo, X.; Li, J.; Li, C; Heng, L.; Dong, Y.; Liu, Z.; Bo, Z.; Tang, B. Z. *Adv. Mater.* **2011**, *23*, 3261−3265. (d) Li, H.; Chi, Z.; Xu, B.; Zhang, X.; Li, X.; Liu, S.; Zhang, Y.; Xu, J. *J. Mater. Chem.* **2011**, *21*, 3760−3767.

(25) Lin, S.-H.; Wu, F.-I.; Tsai, H.-Y.; Chou, P.-Y.; Chou, H.-H.; Cheng, C.-H.; Liu, R.-S. *J. Mater. Chem.* **2011**, *21*, 8122−8128.

(26) (a) Zhang, G.; Lu, J.; Sabat, M.; Fraser, L. *J. Am. Chem. Soc.* **2010**, *132*, 2160−2162. (b) Nguyen, D.; Zhang, G.; Lu, J.; Sherman, E.; Fraser, L. *J. Mater. Chem.* **2011**, *21*, 8409−8415.
(27) (a) Lai, C.-T.; Chien, R.-H.; Kuo, S.-W.; Hong, J.-L. *Macromolecules* **2011**, *44*, 6546−6556. (b) Bhalla, V.; Vij, V.; Dhir, A.; Kumar, M. *Chem.—Eur. J.* **2012**, *18*, 3765−3772. (c) Wang, X.; Hu, J.; Liu, T.; Zhang, G.; Liu, S. *J. Mater. Chem.* **2012**, *22*, 8622−8628. (d) Lu, H.; Su, F.; Mei, Q.; Tian, Y.; Tian, W.; Johnson, R. H.; Meldrum, D. R. *J. Mater. Chem.* **2012**, *22*, 9890−9900.
(28) (a) Zhang, L.-H.; Jian, T.; Wu, L.-B.; Wan, J.-H.; Chen, C.-H.; Pei, Y.-B.; Lu, H.; Deng, Y.; Bian, G.-F.; Qiu, H.-Y.; Lai, G.-Q. *Chem.—Asian J.* **2012**, DOI: 10.1002/asia.201200070. (b) Qian, Y.; Cai, M.; Zhou, X.-H.; Gao, Z. Q.; Wang, X.; Zhao, Y.; Yan, X.; Wei, W.; Xie, L.-H.; Huang, W. *J. Phys. Chem. C* **2012**, DOI: 10.1021/jp212257f. (c) Ishi-i, T.; Ikeda, K.; Kichise, Y.; Ogawa, M. *Chem.—Asian J.* **2012**, DOI: 10.1002/asia.201200136.